



# Simplify your imaging workflows

Make research imaging workflows accessible, traceable, and secure with Athena Software for Core Imaging Facilities.

Thermo Scientific™ Athena Software is a premium imaging data management platform designed for core imaging facilities that support materials science research.

Athena Software ensures traceability of images, metadata, and experimental workflows through an intuitive and collaborative web interface.

Find out more at [thermofisher.com/athena](http://thermofisher.com/athena)

**ThermoFisher**  
SCIENTIFIC

# Acid and Alkali-Resistant Textile Triboelectric Nanogenerator as a Smart Protective Suit for Liquid Energy Harvesting and Self-Powered Monitoring in High-Risk Environments

Liyun Ma, Ronghui Wu, Aniruddha Patil, Jia Yi, Di Liu, Xuwei Fan, Feifan Sheng, Yifan Zhang, Sai Liu, Shen Shen, Jun Wang,\* and Zhong Lin Wang\*

**Industrialization and anthropogenic activities are expected and unavoidable to consummate the current resources of humankind, which also lead to accidents in the laboratory, chemical plants, or other high risk areas that cause severe burns, or even casualties. Increased casualties in such accidents are due to inappropriate safety measures and prevention. Here, a smart anti-chemical protective suit with a bio-motion energy harvesting and self-powered safety monitoring system is demonstrated, which can protect the body from chemical harm, detect sudden chemical spills, monitor human real-time living signals, and trigger alarms in an emergency. Particularly, a fabric triboelectric nanogenerator (F-TENG), which is fabricated by the all-fiber single-electrode triboelectric nanogenerator yarn (SETY), works as the basic elements of the intelligent suit. The SETY with core-shell structured design shows a high sensitivity to the corrosive liquids including acids and alkalis. Furthermore, the working principle of the yarn based nanogenerator that is powered by contacting with acid liquid droplets is demonstrated for the first time. In addition, discretionary thickness, permeability, and any other functionalities are also achieved by taking advantage of the fabric structure. This self-powered smart anti-chemical protective suit equipped with a real time monitoring system will benefit the wearer who works in a very high-risk environment.**

## 1. Introduction

To chase the demand of improved modernization and civilization, anthropogenic activities and industrial development played an unparalleled role. Along with impactful outcomes, the activities become major concern of laboratory accidents,<sup>[1]</sup> chemical plant accidents,<sup>[2]</sup> and special workshop incidents.<sup>[3]</sup> The most common accidents in these events are leakage or splashing of corrosive solutions such as acid and alkali, which not only seriously endangers the health of operators, but also affects public safety in terrible cases.<sup>[4]</sup> Existing coated film protective clothing has poor air permeability, causing operators to feel uncomfortable and unwilling to wear and work for a long time.<sup>[5]</sup> Moreover, the real-time sensing<sup>[6]</sup> about the chemical leakage is necessary for the user to make a timely response strategy and avoid serious consequences.<sup>[7]</sup> Therefore, advanced protective clothing with acid and alkali resistance, good air permeability,

Dr. L. Ma, J. Yi, D. Liu, F. Sheng, S. Shen, Prof. Z. L. Wang  
Beijing Institute of Nanoenergy and Nanosystems  
Chinese Academy of Science  
Beijing 100083, China  
E-mail: zhong.wang@mse.gatech.edu

Dr. L. Ma  
College of Textile and Clothing  
Xinjiang University  
Urumqi 830046, China

Dr. L. Ma, Dr. R. Wu, Y. Zhang, Dr. S. Liu, Prof. J. Wang  
Key Laboratory of Textile Science & Technology  
Key Laboratory of High Performance Fibers & Products  
Ministry of Education  
College of Textiles  
Donghua University  
Shanghai 201620, China  
E-mail: junwang@dhu.edu.cn

Dr. L. Ma, Dr. R. Wu, Dr. A. Patil, X. Fan, Y. Zhang  
College of Physical Science and Technology  
School of Informatics  
Fujian Provincial Key Laboratory for Soft Functional Materials Research  
Xiamen University  
Xiamen 361005, China  
Prof. Z. L. Wang  
School of Materials Science and Engineering  
Georgia Institute of Technology  
Atlanta, GA 30332, USA

 The ORCID identification number(s) for the author(s) of this article  
can be found under <https://doi.org/10.1002/adfm.202102963>.

DOI: [10.1002/adfm.202102963](https://doi.org/10.1002/adfm.202102963)

and good splash sensing function, which not only protects the health of employees from harm, but also enables the wearer to make timely and correct judgments and operations in the event of an accident is urgently needed.

Till now, polytetrafluoroethylene (PTFE) has played an unbeatable role in the polymer industry, as it has good acid and alkali resistance, oxidation resistance, non-toxicity, and other excellent properties, therefore, it is widely used in the mechanical, electronic, and even military fields. Owing to these features, PTFE would be an excellent choice for protective textiles to solve the aforementioned problems. Why in most cases PTFE materials are only used in industrial textiles and seldom used in apparel textiles? The reason is that the small dielectric constant value of PTFE makes it easy to generate static electricity during friction,<sup>[8]</sup> which will result in the failure of normal production of PTFE fabric, let alone high-speed production. Specifically, the static electricity will cause unclear shedding (warp yarn weaving opening), mechanical failures or even major accidents. In this concern, solving the above discussed difficulties of PTFE in the textile processing is a common expectation of in textile industry. The developed methods (emulsion dipping, laminating composite method, and sputter coating)<sup>[8,9]</sup> are mainly based on coating of PTFE materials on the fabric, which will invalidate the fabric washability,<sup>[10]</sup> air permeability,<sup>[11]</sup> comfort,<sup>[12]</sup> style.<sup>[13]</sup> Moreover, the high molecular weight of PTFE makes it difficult to adhere to the fabric surface and the coating on fiber surface is uneven because of Plateau-Rayleigh instability.<sup>[14]</sup> Herein, a high-speed compound spinning method fed by the two-axis system and the structure of the core-sheath composite yarn (i.e., single-electrode triboelectric nanogenerator yarn [SETY]) is first time applied to solve the above mentioned issues. The obtained composite yarn (conductive yarn is used as the core yarn, while the PTFE yarn is the sheath yarn) can transfer the static electricity generated by the PTFE to the conductive yarn in time, so it can be woven after entering the weaving system without static electricity causing unclear shed. More importantly, the yarn can work as a single-electrode triboelectric nanogenerator,<sup>[15]</sup> turning the disadvantage of PTFE that is prone to static electricity into an advantage.

Thereby, a composite all-fibers SETY with anticorrosion, washability, flexibility, functionality, and intelligence has been fabricated at commercial scale. Furthermore, the ultra-low surface energy and the low dielectric constant revealed by PTFE enable SETY to use as self-powered acid and alkali prevention and leakage detections. Moreover, the working principle of the yarn based nanogenerator powered by acid droplets has been clarified for the first time. The deformable SETY can also be applied to monitor the breathing and joint movement information in combination with the special engineering structure (secondary low-twist yarn structure or non-stretchable and stretchable yarn assembly). Beyond this, a bio-motion energy harvesting and self-powered safety monitoring system, which has four functionalities of acid and alkali resistance, self-powered chemical leakage detection, operator vital signs monitoring, as well as real-time remote alarm is established based on the fabric triboelectric nanogenerator (F-TENG). Hence, a protective suit with good air permeability, anti-chemical property, detectability, and intellectuality is efficiently manufactured, which can benefit for people working in laboratory, chemical plant, special workshop, and emergency place.

## 2. Results and Discussion

### 2.1. Smart Anti-Chemical Protective Suit Enabled by SETY and F-TENG

As schematic illustrated in Figure 1a, the smart anti-chemical protective suit which is enabled by F-TENG and its basic element SETY has four functionalities in extreme working environment. First, it has a good acid and alkali resistance functionality compared with ordinary fabrics because of the intrinsic anti-chemical performance of PTFE sheathed SETY.<sup>[16]</sup> As shown in Figure 1a-i, the ordinary fabrics was corroded and damaged by sulfuric acid, but F-TENG remained intact. Second, it can be used for self-powered chemical leakage monitoring (Figure 1a-ii), as obvious signals can be generated when the chemical droplet slapping on the core-shell structured hydrophobic yarn. Third, the smart suit provides a vital sign and motion monitoring function to detect the operator status under dangerous working environment (Figure 1a-iii). Fourth, a real-time remote alarm system has been achieved by tapping the SETY on the protective suit (Figure 1a-iv). The SETY used to prepare F-TENG can be easily and “invisibly” integrated into the textile through a reasonable structural design to monitor various physiological and motion signals, which can be used to make sure that the wearer is alive and safe or not in dangerous situations. The continuous SETY with excellent acid and alkali resistance, energy harvesting and self-powered sensing functions is fabricated by the fancy twisting machine (Figure S1a,b, Supporting Information) based on the high-speed spinning technology of a two-axis feeding system (Figure 1b). This SETY is a core-sheath structure composite yarn by taking the PTFE filament as the sheath yarn and conductive polyamide yarn as the core yarn. As shown in Figure 1c, SETY is well formed by the even wrapping of the PTFE filament on the conductive yarn. Based on the good flexibility of SETY, it can be used for knotting, sewing, weaving, etc. (Figure 1d,e; Figure S1c–f, Supporting Information). At the same time, the SETY can be adapted to the processing of mechanical weaving manufacturing, and was successfully woven into fabrics with different structures (Figure 1c). The as-weaved F-TENG from SETY has a smooth surface with excellent hydrophobicity and acid and alkali resistance (Figure 1f,g).

### 2.2. Structure and Performance Characterization of the SETY

As a basic unit of the F-TENG, the mechanical, electrical, and other physical properties of the SETY have a significant influence on the performance of F-TENG. As shown in Figure S2, Supporting Information, the SETY has a fineness of 192.60 tex with a uniform surface. The SETY's mechanical properties which affect the yarn weavability and durability are studied from both experimental and theoretical aspects. As shown in the tensile stretching curve (Figure S3, Supporting Information), both conductive yarn (core yarn) and PTFE yarn (wrapped yarn) show viscoelastic properties, and the breaking strain of SETY (composite yarn) is close to that of the core yarn.<sup>[17]</sup> This is because the core yarn is stretched under force during the stretching process of composite yarn, while the wrapped yarn



**Figure 1.** Schematic illustration of SETY, F-TENG, and intelligent anti-chemical protective suit. a) Schematic of anti-chemical protective suit, which has four functions of anti-chemical property, chemical leakage monitoring, vital signal monitoring, and real-time alarm system. b) Schematic of SETY fabricating process. c) Photograph and SEM image of SETY and F-TENG fabricating process. d,e) Images of SETY. f,g) Images of F-TENG.

presents a conformation of being unwound after being stressed, as it gradually changes from the spiral conformation to straight conformation without elongation. Based on the above discussion and the mechanical characteristics, a three-element mechanical model is selected to fit the mechanical curve,<sup>[18]</sup> and

the fitting correlation coefficient is as high as 0.997 (Figure 2a). The mechanical model provides guidance for the mechanical performance of the composite self-powered yarn sensor.

Electrical output performance is another significant physical property of SETY, which directly affects the performance of a

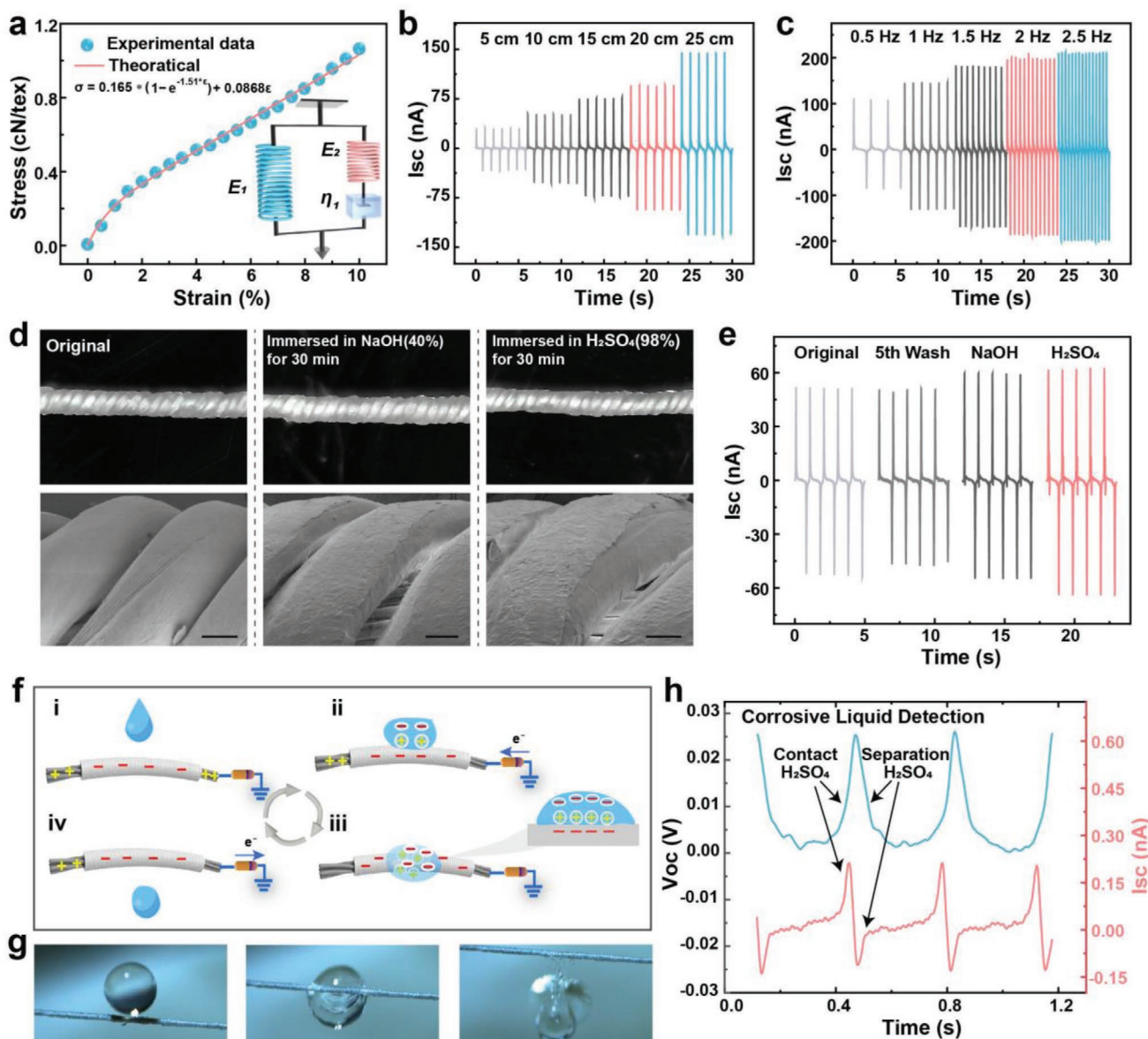


**Figure 2.** Performance of SETY. a) Comparison of the experimental stress–strain curves of SETY and the theoretically fitting results by viscoelastic model (inside of chart,  $\sigma$  refers to the stress on SETY,  $\epsilon$  refers to the strain of SETY,  $E_1$  and  $E_2$  refer to the elastic modulus of springs representing the sheath and the core of SETY, and  $\eta_i$  refer to the viscous coefficients of the dashpots representing the core of SETY). b,c) Short-circuit current of SETY with different length and frequency. Acid and alkali resistance performance test: d) Surface of sheath yarn is slightly corroded, but there is no damage inside the sheath and core yarn (scale bar, 50  $\mu$ m). e) Electrical output performance after water washing and acid and alkali soaking. f) Demonstration of the working principle for SETY. g,h) Photographs and electrical output of droplet contacting and separating from SETY.

single yarn (SETY) as a self-powered sensor and the electrical properties of subsequent fabrics.<sup>[19]</sup> Therefore, the working principle of SETY during contact and separation (Figure S4, Supporting Information) was analyzed and the potential distribution diagram was simulated by COMSOL (Figure S5, Supporting Information).<sup>[20]</sup> Driven by the feasibility of the working principle of SETY, the electrical properties of SETY were further analyzed. As shown in Figure 2b,c and Figure S6, Supporting Information, the electrical output is enhanced with a yarn length of 5 to 25 cm; the short-circuit current ( $I_{sc}$ ) increases with the

acceleration of the testing frequency (0.5 to 2.5 Hz) and increment of the force load (5 to 15 N), indicating good electric output performance of the SETY. At the same time, the 0.1  $\mu$ F capacitor can be charged to 3 V by a single yarn in about 30 s and the output power reaches the maximum value at 400 M $\Omega$ .

Smart anti-chemical protective suits should have good performance of washability, acid and alkali resistance, and hydrophobicity of basic element (SETY). The washing resistance and acid and alkali resistance of the SETY are characterized and showed in Figure S7 and Video S1, Supporting Information. From the

SEM images (Figure 2d) and the electrical output properties (Figure 2e) of the SETY after washing and immersion in acid and alkali solution, it can be seen that the electrical performance slightly decreased after washing five times. On the contrary, the electrical output of the SETY did not decrease after immersion in acid and alkali solution but increased. This is because when the acid and alkali solution etch the surface of PTFE filaments, the specific surface area (wrinkles) increases,<sup>[21]</sup> which makes it easier for the electrons moving when the dielectric material is in contact. Moreover, the hydrophobicity of SETY was tested by an in-situ observation method. As shown in Figure S8 and Video S2, Supporting Information, when the SETY was moved upward to completely contact the water drop, and then moved downward to separate with the water drop, the water droplet was not attached on SETY and restored to its original shape, which shows the excellent hydrophobicity of SETY.

Based on the above-mentioned performances, that is, acid and alkali resistance, and hydrophobicity, SETY can be used for harvesting energy from droplet (water, acid, and alkali droplet), or monitoring droplet leakage. In the initial stage, the uncharged droplet ( $H_2SO_4$ ) contact and electrify the uncharged PTFE yarn (the outer layer of the SETY), making the PTFE negatively charged and the droplet positively charged.<sup>[22]</sup> With a large number of droplets continuously contacting and separating with PTFE, the negative charge on the surface of the PTFE keeps increasing until reaching a saturation.<sup>[23]</sup> Subsequent droplets fall on the PTFE saturated with negative electricity, and the anions and cations in the droplets will migrate under the action of an electric field (electrostatic induction), forming an electrical double layer (EDL) on the surface of the PTFE.<sup>[24]</sup> The working principle of the energy harvesting model by the contact and separation of droplets and SETY has been illustrated in Figure 2f,g. More specifically, in the initial stage (Figure 2f-i), the PTFE yarn has a negative charge, the conductive yarn has a positive charge, therefore, the SETY is neutral as a whole. In the second stage (Figure 2f-ii), when the  $H_2SO_4$  droplet comes to contact with the PTFE yarn, the negative charge on the yarn will attract the oppositely charged ions of the  $H_2SO_4$  droplet, thereby forming another positively charged ion. This electrical double layer (EDL) creates a positive electron potential difference, so the electrons will be transferred from the ground to the conductive yarn (electrode) until a new equilibrium (the third stage, Figure 2f-iii) is reached. During the process, an instantaneous positive current was produced. When the  $H_2SO_4$  droplet leaves the PTFE yarn, a negative potential difference is formed between the ground and the conductive yarn. Electrons will move to the ground from the conductive yarn, and another new equilibrium will be achieved (Figure 2f-iv). When the droplets periodically contact the PTFE film, continuous electrical output will be obtained. As demonstrated in Figure 2h and Figure S9, Supporting Information,  $H_2SO_4$ , NaOH and water solution was used to test SETY's solid-liquid contact electrification performance. The measurement result is accordance with the described working mechanism, namely, when  $H_2SO_4$  is in contact with SETY (Figure 2h), an upward  $V_{oc}$  signal is generated, and when  $H_2SO_4$  and SETY is separated, a downward  $V_{oc}$  signal is generated. For the current signal, an upward peak is generated during contact and a downward peak during separation.

### 2.3. Structure and Performance Characterization of the F-TENG

Although PTFE has a good mechanical property, acid and alkali resistance performance, and a good performance stability, it is difficult to fabricate into textiles due to the weaving shed clinging caused by the friction induced static electricity. More specifically, in the weaving process (take weaving as an example), the shed composed of warp yarns is controlled by the heald frame to open in order (Figure 3a). When the PTFE filament yarn is used as the warp yarn, the shed tends to be unclear due to the high static electricity between each other (Figure 3b-i). Thus, the weaving structure of the desired woven fabric is not consistent with the realized pattern (Figure 3b-ii), which ultimately leads to defects on the fabric surface. Here, with the core-sheath composite yarn structure which composed of PTFE filaments and conductive yarns, the above problems are solved. The composite yarn (SETY) can eliminate static electricity by the conductive yarn and form a clear shed during weaving (Figure 3c-i; Figure S10a, Supporting Information), and prepare the programmed fabric (Figure 3c-ii, d; Figure S10b,c, Supporting Information). The composite fabric prepared by this method not only maintains the excellent properties of PTFE material, such as hydrophobicity, acid and alkali resistance, etc., but also has energy harvesting and sensing functions without destroying the original properties of the fabric.

According to the application scenarios and requirements, the fabrics can be designed into multiple weaves.<sup>[25]</sup> Simple lifting plans adjustment and design can engineer the fabric structure to control thickness and air permeability (Figure S11, Supporting Information), thereby achieving the various applications of clothing textiles. Here, four kinds of fabric structures, that is, plain, twill, satin, and honeycomb structured fabrics, were weaved by using the SETYs as warp and weft yarns. It turns out that the plain weave structured fabric has the smallest thickness while the honeycomb one has the biggest (Figure S11a, Supporting Information). Furthermore, the highest air permeability is recorded in case of plain weave fabric (Figure S11b, Supporting Information) that is, up to  $862.26\text{ mm s}^{-1}$ , whereas the lowest ( $270.20\text{ mm s}^{-1}$ ) is recorded for the 3/3 twill fabric. These results showed that the F-TENG has a good and discretionary air permeability, which meets the requirements for clothing textiles.

At the same time, for F-TENGs with different weave structures, although the sheath yarn of SETY is all hydrophobic, the contact angles of the obtained F-TENGs are slightly different (Plain structure fabric:  $138.97^\circ$ , 3/3 Twill structure fabric:  $132.85^\circ$ , 2/1 Twill structure fabric:  $134.48^\circ$ ) due to the different arrangement of the yarns (Figure 3e; Figure S12, Supporting Information). The hydrophobicity of the whole fabric was tested by static dipping method, dynamic spraying, and shaking method.<sup>[26]</sup> When the cotton fabric and F-TENG with the same size are immersed in dyeing water (Figure 3f; Video S3, Supporting Information), the cotton fabric immediately absorbs water and turns red while F-TENG shows an excellent water repellency. After taking F-TENG out of the water, the surface of F-TENG was not stained or discolored, and no red liquid remained on the surface. The tested result of the hydrophobicity of the fabric by using spraying method (Figure S13 and Video S4, Supporting Information) is consistent with the result

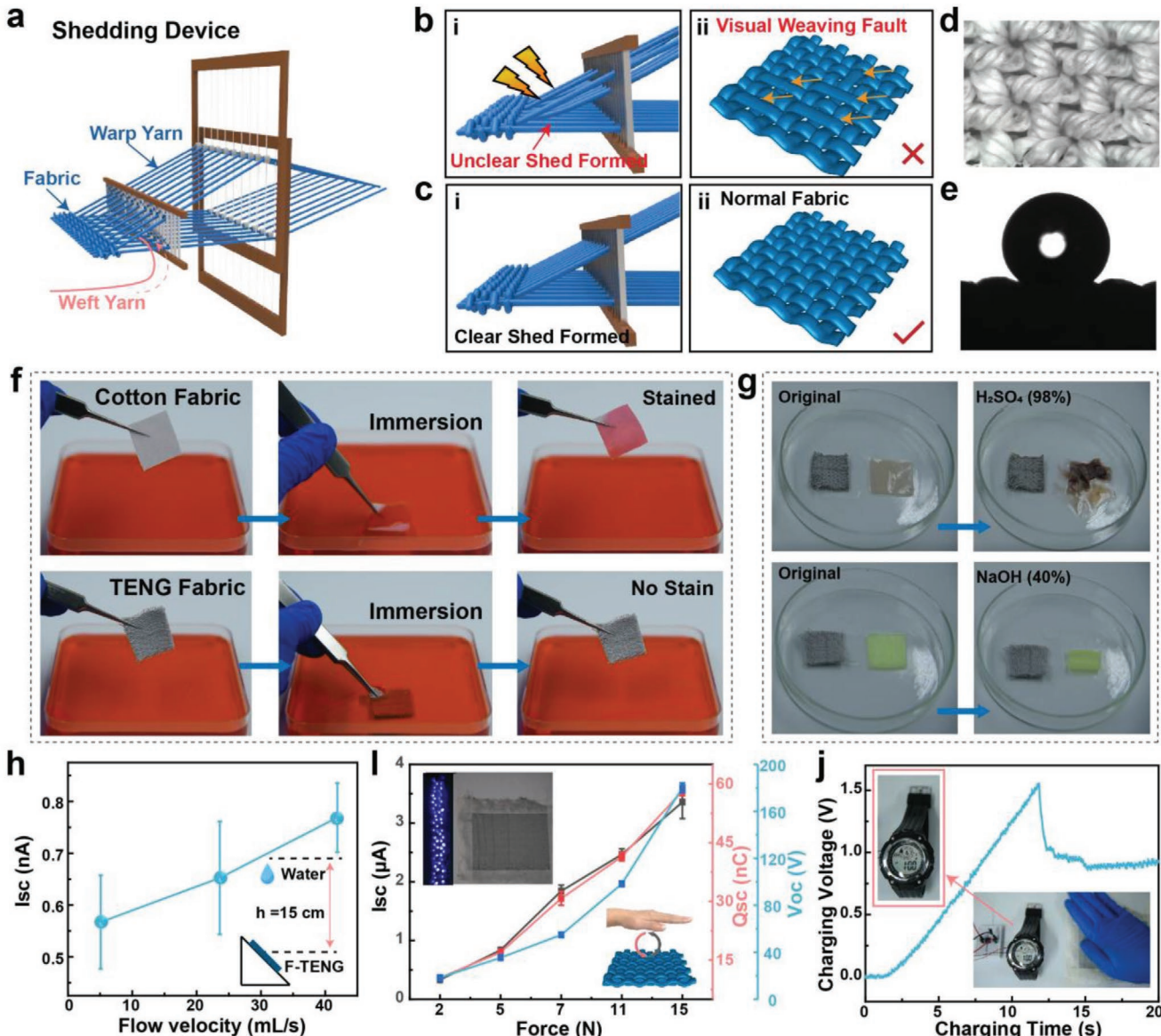


**Figure 3.** Performance and application of F-TENG. a) Schematic diagram of shedding device of weaving machine. b) Due to the static electricity of PTFE filaments, it is easy to form an unclear shed during weaving processing, and finally cause visual weaving faults. c) The composite yarn (SETY) can effectively eliminate static electricity, form a clear shed during weaving processing, and weave into a fabric with a good surface. d) Photograph of plain structure F-TENG. e) Hydrophobicity of the plain structure F-TENG. f) Photographs showing the procedures of dipping F-TENG and cotton fabric into colored water. g) Optical photographs showing the acid resistance and alkali resistance of F-TENG. h) Electrical output of water droplets contacting and separating from F-TENG. i) Electrical output of bio-motion energy, which is enough to lighting up 58 LEDs. j) F-TENG harvest bio-motion energy to charge a capacitor for driving an electrical watch.

of dipping test. It can be seen from the Video S5 and Figure S14, Supporting Information, when 5 mL of water droplet was dropped on the fabric, the water droplet was not absorbed or dispersed by the fabric during shaking the fabric, and the water is dumped and separated from the fabric when tilting the fabric. Thus, according to the results of dynamic and static characterization, it has proved that the fabric has good hydrophobicity.

As the acid and alkali resistance is a very important performance of F-TENG for anti-chemical protective suit, further characterizations are carried out. Here, deionized water, coffee, tea, sulfuric acid solution, and sodium hydroxide solution were

dropped on F-TENG (Figure S15, Supporting Information) for 5 minutes, it turns out that the F-TENG was not damaged by acid (or alkali) solution and its appearance was remained as original. Moreover, another characterization method with immersing the whole piece of F-TENG and the reference cotton fabric in 98%  $H_2SO_4$  solution and 40% NaOH solution was carried out. The fabrics were observed under liquid-carrying conditions. It was found that the cotton fabric was gradually carbonized while F-TENG barely changed; after scraping the fabrics with tweezer, the cotton fabric disintegrated while F-TENG kept its original appearance (Figure 3g; Figure S16 and Video S6,

Supporting Information). Therefore, the F-TENG fabric exhibits good acid and alkali resistance performance and shows potentials in anti-chemical protective suit.

Based on the working principle of SETY in Figure 2f and the hydrophobicity performance, the F-TENG can also be used for water droplet energy harvesting or liquid leakage detecting. As shown in Figure 3h, the energy generating abilities under different dropping speeds are tested. It shows that the slow-dropping water droplets contacting and separating from the F-TENG can generate power of 0.55 nA ( $I_{sc}$ ), and it keeps increasing with the enhanced dropping speed. The  $V_{oc}$  and  $Q_{sc}$  values and the stability of electric signal when alkali liquid contacts and separates from the F-TENG were also tested (Figure S17, Supporting Information). In addition to harvesting water droplet energy, the fabric also has the ability to collect bio-energy. As a clothing textile, when the body parts, such as hand, arm, leg, or feet are contacted with (or separated from) the F-TENG, it can generate considerable energy. When hand taps the F-TENG with a force of about 2 N, power of 0.33  $\mu$ A, 10.49 nC, and 18.37 V can be generated (Figure 3i). With the increase of hand applied force, the converted energy also rises. When contacting the fabric with a force of about 15 N, the value of  $I_{sc}$ ,  $V_{oc}$ , and  $Q_{sc}$  can be reached as high as 3.36  $\mu$ A, 58.21 nC, and 180.06 V. Moreover, it can be seen from the inset of Figure 3i and Video S7, Supporting Information, that 58 LEDs can be driven by this bio-energy. Through the bio-motion energy harvesting, the F-TENG can charge a capacitor to drive an electronic watch (Figure 3j; Video S8, Supporting Information).

#### 2.4. Bio-Signal Monitoring by the SETY

Real time monitoring of human physiological signal in extreme environments is another essential feature of the anti-chemical protective suit. In this concern, 1D yarn will offer various functions simply by changing fiber materials, designing yarn's structure or adjusting the parameters of the yarn.<sup>[27]</sup> On account of the conception, a low-twist secondary composite yarn (LTSY) by taking SETY as sheath yarn and spandex as core yarn was prepared by adjusting the twist (Figure 4a). During the LTSY fabrication processing, if the spandex yarn is wrapped by SETY under the condition of tension, when LTSY gets off from the machine, SETY will form raised loops on the spandex surface. The SETY is separated from the spandex when the LTSY is not stressed, but when the LTSY is stretched, the spandex becomes longer with tensile force while the wrapped SETY will not be stretched. Therefore, as the LTSY is stretched, SETY gradually contacts with spandex and generates a downward  $I_{sc}$  signal, and when LTSY returns to its original shape, SETY will separate from spandex and produce an upward  $I_{sc}$  signal. Based on the above structure features, this LTSY can realize energy harvesting function by stretching without external objects, and it can also be used as a self-powered stretching sensor (Video S9, Supporting Information). Here, LTSY was fixed on the chest of cloth to monitor the human respiration condition. When a volunteer inhales, the chest cavity becomes larger and LTSY is stretched, and SETY produces a downward  $I_{sc}$  signal; when the volunteer exhales, the chest cavity becomes smaller and LTSY returns to its original shape, and SETY produces an upward

$I_{sc}$  signal. These upward and downward signals change come from the respiration information, which can be used to judge breathing status (alive or dead). The volunteers were detected for different breathing conditions: normal breathing, respiratory arrest, tachypnea, and deep breathing, which are judged by respiration rate and respiration depth (Figure 4b). For respiration rate, it can be calculated by the repetitions number of the signal's fluctuation within a unit time. Breathing rate indicate slow breathing or tachypnea situation. When the human respiration signal is not fluctuated for a long time, it means that the respiratory has stopped, which indicates a need of emergency treatment. For respiration depth, it can be distinguished by the signal value, that is, the signal value of deep breathing is large, and the signal value of normal breathing is relatively small. These physiological signals will help to real-time monitor the operators' health information.

Besides, the SETYs were demonstrated to be successfully developed as a movement monitoring device through the combination of yarn and fabric structure. In Figure 4c, SETYs were sewed on a stretchable fabric. When the fabric is in the initial state, SETY and the fabric are separated. When the flexible fabric substrate stretched or bended, SETY can contact the fabric and generate a contact signal. When the fabric returns to its original state, SETY generates a separation signal (Figure 4d–g). As the fabric on the joint part will be stretched during bending, the concept of SETY combined with stretchable substrate can be applied to detect the human bending motions. Based on above discussion, we have designed intelligent protectors, namely, smart wrist bracer, smart elbow bracer, smart knee bracer, and smart ankle bracer (Figure 4h–k; Figure S18, Supporting Information). As illustrated in Figure 4l–o, both  $I_{sc}$  and  $V_{oc}$  signals can be used to test joint movement. When volunteer's wrist is bent at three angles of 15°, 30°, and 60°,  $V_{oc}$  signals with different amplitudes will be generated. And when volunteers bend their arms from 0° to 135°, the  $I_{sc}$  signal value will gradually increase, namely, the larger the bend angle, the larger the contact area of the SETY with the fabric substrate and the larger the electrical output  $I_{sc}$  signal (Video S10, Supporting Information). Similarly, the smart knee bracer and smart ankle bracer were used to test the movement of the knee and ankle joints. These intelligent protectors can be used to accurately detect the worker joint movement by judging the sensing signals. Therefore, it can also be integrated into protective suit to detect the human body movement and track the trajectory of those who are working in the dangerous environment.

#### 2.5. Smart Anti-Chemical Protective Suit

Based on the discussion above, F-TENG can be used in special high-risk environments based on its multi-functionality of excellent acid and alkali resistance, chemical leakage detecting as well as real time human physiological and motion signal detection. As showed in Figure 5a, wearing the protective clothing with acid and alkali resistance and real-time monitoring function can prevent the corrosion and harm of acid and alkali liquids to operator. In accidents, when acidic (or alkaline) liquids spill out, the splashed droplets fall on the operator's protective clothing, subsequently, F-TENG

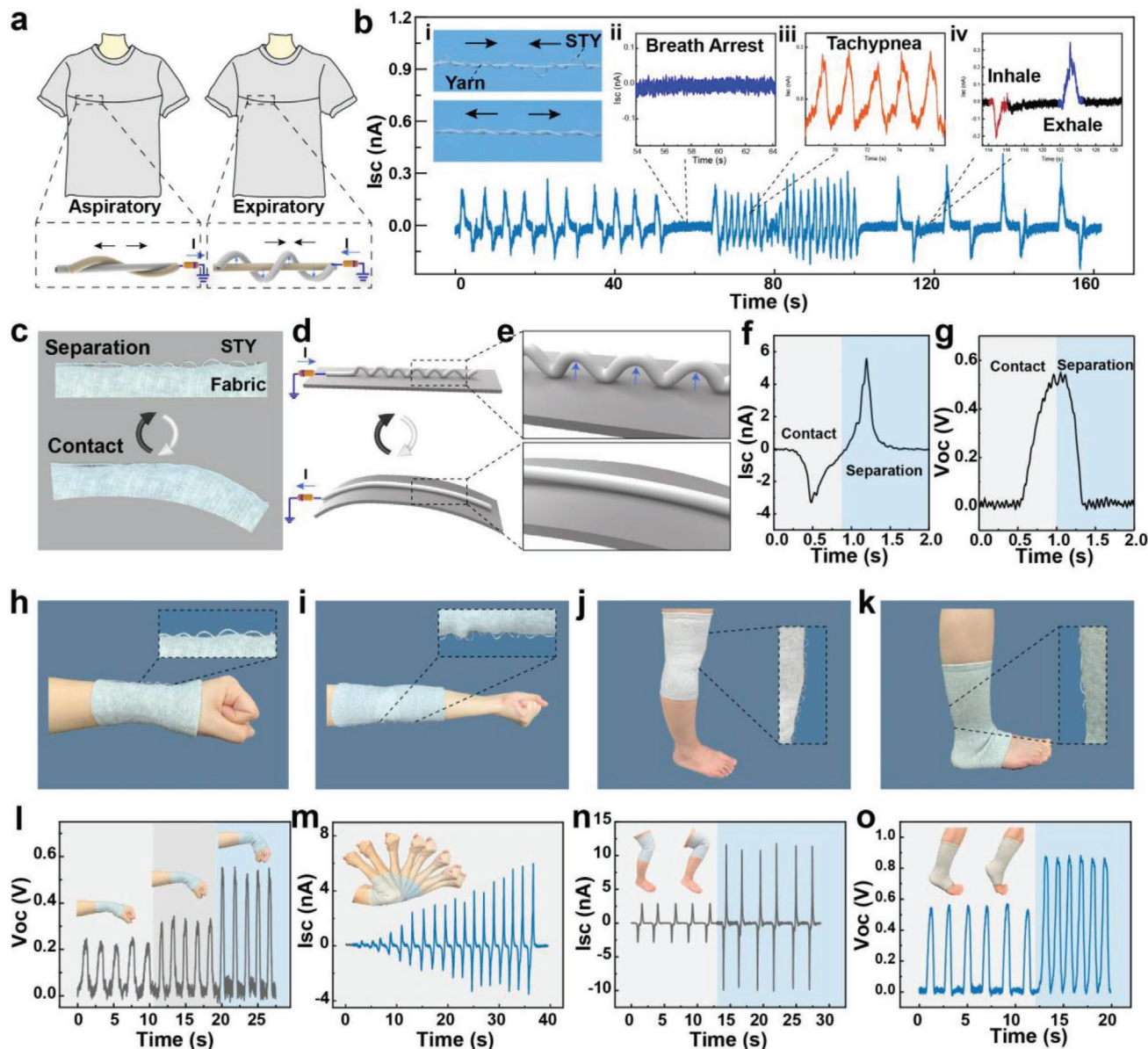


**Figure 4.** Applications of SETY in operator physiological signal detection and motion tracking. a) Working principle and schematic diagram of SETY for monitoring respiration situation. b) Monitoring data for normal respiratory, respiratory arrest, tachypnea, and deep breath. Motion measurements at various positions and analysis of the signals: c–g) Working principle diagram and electrical output performance of SETY for monitoring bending movement. Photographs and measurement data of h,l) smart wrist bracer, i,m) smart elbow bracer, j,n) smart knee bracer, and k,o) smart ankle bracer equipped with SETY.

integrated clothing will generate a signal (Video S11, Supporting Information) which will collect in the form of real-time voltage data by the monitoring platform in a CCTV room (Figure 5a), which will be processed by the signal processor to issue a warning signal, and other staff can provide timely help for the operator.

Therefore, we sew twill structured F-TENG and SETY on the chest and arm of a normal fabric suit, respectively, which would reveal the applicability of F-TENG and SETY. For safety reasons, the suit sample was put on a dummy (Figure 5b,d). When the F-TENG is touched, the detection platform will send out an

alarm “SOS” signal (Figure 5b,c), and when SETY is touched, the detection platform will send out a normal “Okay” signal (Figure 5d–f; Video S12, Supporting Information). F-TENG with plain structure is also applied for the alarm system (Figure S19, Supporting Information), and it shows the same result as twill structured F-TENG. When the acid solution is poured on the F-TENGs, an alarm signal is issued, the F-TENGs are not damaged, and the alarm signal can still be issued when touching the F-TENGs again. However, fabrics with other materials on the suit are corroded and damaged (Video S13, Supporting Information).

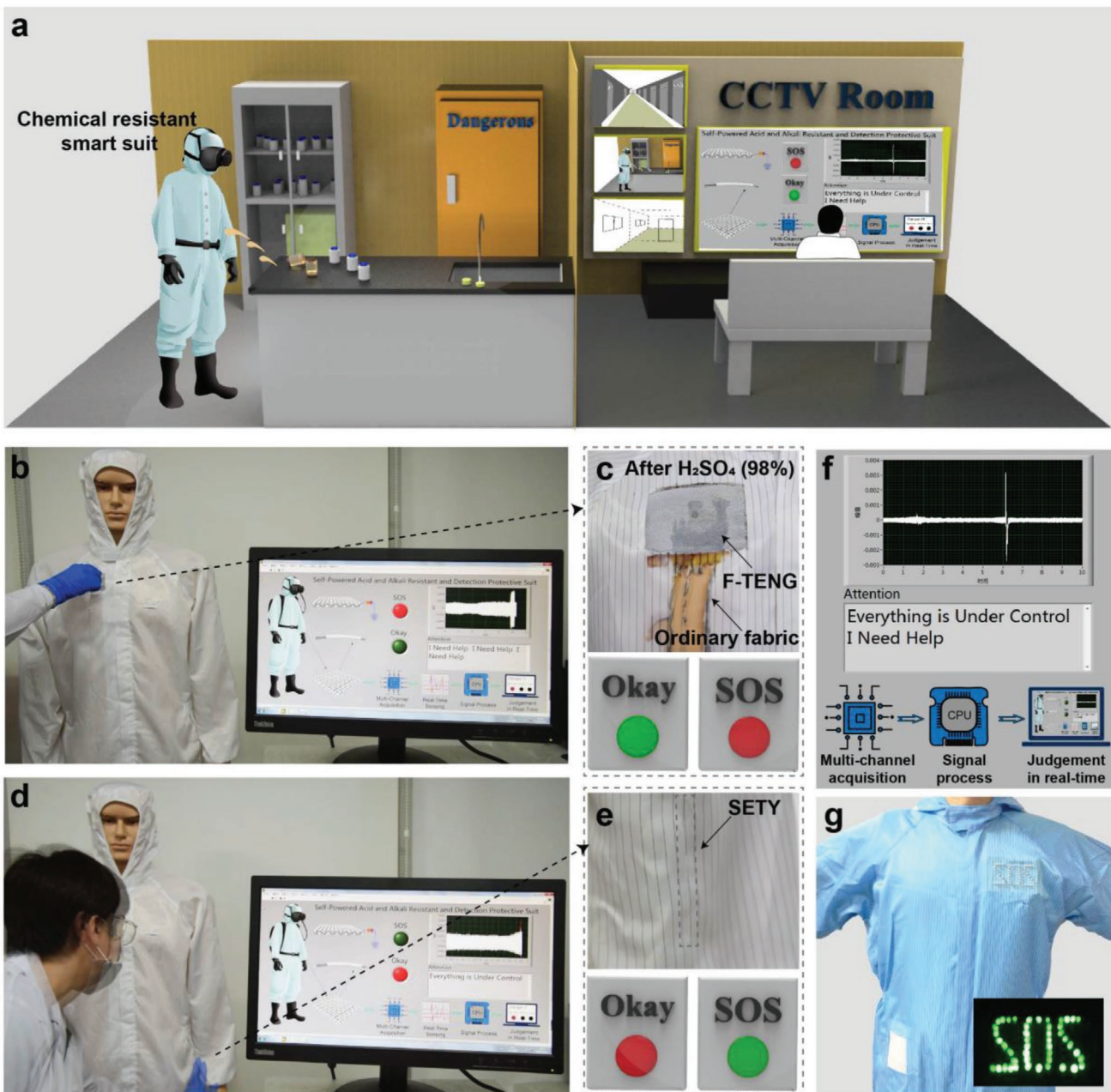


**Figure 5.** Application of the smart anti-chemical protective suit to a bio-motion energy harvesting and self-powered safety monitoring system. a) Demonstration and application scenarios of self-powered anti-chemical protective monitoring suit. b–e) Smart self-powered monitoring suit system, which fabricated by SETY, F-TENG, and ordinary suit. The “okay” signal is generated when the SETY on arm is touched, and the “SOS” signal is generated when the sulfuric acid is splashed on the F-TENG, and the F-TENG is not damaged after encountering sulfuric acid, but the substrate fabric is damaged. f) Scheme and signal display of the monitoring system. g) Demonstration of lighting up LEDs marked as word “SOS” by tapping the F-TENG sewed on the suit.

In addition, based on the good energy harvesting ability of the F-TENG, the smart anti-chemical protective suit can also be used to improve the rescue rate in extreme dark environment. In detail, when there is a lot of smoke in the environment, it is difficult to breathe and one cannot cry for help, by tapping the cloth worn to light up the “SOS” signal, it can attract the attention of rescuers and to get timely rescue (Figure 5g; Figure S20 and Video S14, Supporting Information).

### 3. Conclusion

In summary, a smart anti-chemical protective suit with good air permeability, anti-chemical property, detectability, and intellectuality is fabricated to protect the wearer from chemical spillage accidents in the laboratory, chemical plant, and special workshops. This smart suit is equipped with a bio-motion energy harvesting and self-powered safety monitoring system, which

has acid and alkali resistance, self-powered chemical leakage detection, operator vital signs monitoring, and real-time remote alarm functionalities. A full-fiber SETY with unlimited length, anticorrosion, wash-ability, flexibility, functionality, and intelligence is the fundamental of this suit. Moreover, the working principle of the yarn based nanogenerator powered by droplets has been clarified and discussed for the first time. The LSTY is designed by the special engineering structure design protocol, and proposed with good applicability for real time physical health monitoring. What's more, based on the concept of turning waste into treasure, taking advantage of the core-sheath structure yarn, the electrostatic charge accumulated by the PTFE material due to friction is transferred in time through the core yarn, so that the PTFE material can be woven into a fabric (F-TENG), which solves the application problem of PTFE materials in clothing fabrics. In one word, this smart anti-chemical protective suit and the self-powered safety monitoring system fabrication strategy is offering promising applications in very high-risk environment, and will directly benefit those working in very high-risk chemical environments.

## 4. Experimental Section

**Materials:** PTFE yarn (yarn fineness was 200D) was purchased from Shandong Senrong New Materials Co., Ltd, China. Conductive polyamide yarn was brought from Qingdao Zhiyuan Xiangyu Functional Fabric Co., Ltd., China. The cotton fabric was purchased from Renzhiyun flagship store on Taobao.

**Fabrication of SETY:** The sheath layer yarn (PTFE yarn) was transferred to the hollow yarn bobbin from commercial bobbin by QFB650 yarn pressing machine. As shown in Figure 1, hollow yarn bobbin and core yarn were mounted on empty core fancy twisting machine (QFB730K), and then, turned on after setting parameters. Continuous SETY was produced by above steps.

**Fabrication of F-TENGs:** Semi-automatic weaving machine (SGA598, Jiangyin Tongyuan Textile Machinery Co., Ltd.) was used for weaving F-TENGs. First, SETY was arranged on loom to prepare as warp yarn; second, SETY was wrapped around the shuttle as filling yarn; finally, lifting plan of the fabric (F-TENG) structure was input into the control computer of the loom (Figure S9, Supporting Information) and the weaving process started.

**Measurements and Characterizations:** The morphologies of SETY were analyzed by scanning electron microscopy (TM3000, Hitachi Group-Japan) and electron microscope (Dongguan Bigao Electronic Products Co., Ltd.). The XL-1A yarn strength elongation tester (Shanghai Xinxian Instrument Co., Ltd.) was used to test mechanical properties of SETY. Evenness of SETY was measured by blackboard yarn examining machine (YG381) and measuring reel machine (YG086C). SETY was wound on a shelf and washed in a container to test washing resistance of SETY. A high-speed camera (Photron Mini AX200, Japan) was used to observe the contact and separation situation of the droplets with SETY (or F-TENG). Hydrophobicity of SETY and its fabric was characterized by dynamic contact angle tester (DSA100, Dataphysics, Germany). Sulfuric acid (98%  $H_2SO_4$ ) and sodium hydroxide (40% NaOH) solution were used as acidic and alkaline solutions for testing the acid and alkali resistance of SETY and its fabrics. The fabric thickness and air permeability were measured by digital thickness gauge (YG141D-11) and air permeability tester (YG461E, Wenzhou Fangyuan Instrument Co., Ltd.), separately. Electrical output performances of samples were recorded by electrometer (Keithley 6514). The TENG fabric and yarn were pasted on the paper to test the electrical properties (unless otherwise specified, the test condition was 1 Hz frequency and 15 N force). The data collected in human participants study (physiological signal detection and motion tracking) were approved by volunteers and the consent forms were signed.

## Supporting Information

Supporting Information is available from the Wiley Online Library or from the author.

## Acknowledgements

L.M. and R.W. contributed equally to this work. This work was supported by the National Key Research and Development Program of China (2016YFA0202704) and the Fundamental Research Funds for the Central Universities of China (Grant Nos. 2019061105). The authors acknowledge Professor Chen Xiangyu and Dr. Zhan Fei for insightful discussions.

## Conflict of Interest

The authors declare no conflict of interest.

## Data Availability Statement

Research data are not shared.

## Keywords

anti-chemical fabric triboelectric nanogenerator, bio-energy harvesting device, self-powered sensor, triboelectric yarn

Received: March 27, 2021

Revised: May 11, 2021

Published online:

- [1] C. Y. Zhu, S. Tang, Z. L. Li, X. T. Fang, *Saf. Sci.* **2020**, *130*, 104877.
- [2] C. Zhu, J. Zhu, L. Wang, M. S. Mannan, *J. Loss Prev. Process Ind.* **2017**, *50*, 397.
- [3] H. A. Aziz, A. M. Shariff, R. Rusli, K. H. Yew, *Process Saf. Environ. Prot.* **2014**, *92*, 423.
- [4] a) M. T. Markiewicz, *Environ. Sci. Pollut. Res.* **2020**, *27*, 18269; b) M. Chen, Y. Wu, K. Wang, H. Guo, W. Ke, *Process Saf. Prog.* **2020**, *39*, e12150.
- [5] J. D. Shi, S. Liu, L. S. Zhang, B. Yang, L. Shu, Y. Yang, M. Ren, Y. Wang, J. W. Chen, W. Chen, Y. Choi, X. M. Tao, *Adv. Mater.* **2020**, *32*, 1901958.
- [6] a) J. L. Chen, X. J. Wen, X. Liu, J. Q. Cao, Z. H. Ding, Z. Q. Du, *Nano Energy* **2021**, *80*, 105446; b) L. Y. Ma, Q. Liu, R. H. Wu, Z. H. Meng, A. Patil, R. Yu, Y. Yang, S. H. Zhu, X. W. Fan, C. Hou, Y. R. Li, W. Qiu, L. F. Huang, J. Wang, N. B. Lin, Y. Z. Wan, J. Hu, X. Y. Liu, *Small* **2020**, *16*, 2000203; c) R. H. Wu, L. Y. Ma, A. B. Patil, C. Hou, Z. H. Meng, Y. F. Zhang, X. Y. Liu, W. D. Yu, *Text. Res. J.* **2019**, *89*, 5144; d) Y. Zhang, C. Chen, Y. Qiu, L. Ma, W. Qiu, R. Yu, W. Yu, X. Y. Liu, *Adv. Funct. Mater.* **2021**, *31*, 2100150.
- [7] a) D. A. Huh, E. H. Huh, S. H. Byeon, J. R. Sohn, K. W. Moon, *Int. J. Environ. Res. Public Health* **2019**, *16*, 3271; b) Z. L. Wang, *ACS Nano* **2013**, *7*, 9533.
- [8] T. Y. Kumeeva, N. P. Prorokova, I. V. Kholodkov, V. N. Prorokov, A. G. Buyanova, N. M. Kabaeva, L. V. Gumileva, I. G. Barakovskaya, R. U. Takazova, *Russ. J. Appl. Chem.* **2012**, *85*, 144.
- [9] a) F. Huang, Q. Wei, Y. Liu, W. Gao, Y. Huang, *J. Mater. Sci.* **2007**, *42*, 8025; b) F. Wang, L. Feng, G. Li, Z. Zhai, H. Ma, B. Deng, S. Zhang, *Polymers* **2019**, *11*, 1748.

- [10] a) X. Shi, Y. Zuo, P. Zhai, J. H. Shen, Y. Y. W. Yang, Z. Gao, M. Liao, J. X. Wu, J. W. Wang, X. J. Xu, Q. Tong, B. Zhang, B. J. Wang, X. M. Sun, L. H. Zhang, Q. B. Pei, D. Y. Jin, P. N. Chen, H. S. Peng, *Nature* **2021**, 591, 240; b) W. J. Fan, Q. He, K. Y. Meng, X. L. Tan, Z. H. Zhou, G. Q. Zhang, J. Yang, Z. L. Wang, *Sci. Adv.* **2020**, 6, eaay2840.
- [11] a) L. Y. Ma, R. H. Wu, S. Liu, A. Patil, H. Gong, J. Yi, F. F. Sheng, Y. Z. Zhang, J. Wang, J. Wang, W. X. Guo, Z. L. Wang, *Adv. Mater.* **2020**, 32, 2003897; b) X. M. Tao, *Acc. Chem. Res.* **2019**, 52, 307.
- [12] a) Q. Qiu, M. M. Zhu, Z. L. Li, K. L. Qiu, X. Y. Liu, J. Y. Yu, B. Ding, *Nano Energy* **2019**, 58, 750; b) W. Weng, J. J. Yang, Y. Zhang, Y. X. Li, S. Y. Yang, L. P. Zhu, M. F. Zhu, *Adv. Mater.* **2020**, 32, 1902301; c) S. Liu, K. Ma, B. Yang, H. Li, X. M. Tao, *Adv. Funct. Mater.* **2020**, 2007254, <https://doi.org/10.1002/adfm.202007254>.
- [13] a) G. R. Chen, Y. Z. Li, M. Bick, J. Chen, *Chem. Rev.* **2020**, 120, 3668; b) X. A. Zhang, S. J. Yu, B. B. Xu, M. Li, Z. W. Peng, Y. X. Wang, S. L. Deng, X. J. Wu, Z. P. Wu, M. Ouyang, Y. H. Wang, *Science* **2019**, 363, 619.
- [14] P. W. Wang, J. J. Zhou, B. J. Xu, C. Lu, Q. A. Meng, H. Liu, *Adv. Mater.* **2020**, 32, 2003453.
- [15] a) L. Y. Ma, M. J. Zhou, R. H. Wu, A. Patil, H. Gong, S. H. Zhu, T. T. Wang, Y. F. Zhang, S. Shen, K. Dong, L. K. Yang, J. Wang, W. X. Guo, Z. L. Wang, *ACS Nano* **2020**, 14, 4716; b) J. Xiong, J. Chen, P. S. Lee, *Adv. Mater.* **2020**, 33, 2002640; c) T. Jin, Z. D. Sun, L. Li, Q. Zhang, M. L. Zhu, Z. X. Zhang, G. J. Yuan, T. Chen, Y. Z. Tian, X. Y. Hou, C. Lee, *Nat. Commun.* **2020**, 11, 5381.
- [16] S. Liu, S. Cui, Z. Qin, X. Zhang, Y. Zhao, Y. Zhao, H. Guo, *Chem. Eng. Technol.* **2019**, 42, 1027.
- [17] A. M. Manich, P. N. Marino, M. D. De Castellar, M. Saldivia, R. M. Sauri, *J. Appl. Polym. Sci.* **2000**, 76, 2062.
- [18] W. Yu, *Textile Materials*, China Textile Press, Beijing, China **2018**.
- [19] Z. L. Wang, J. Chen, L. Lin, *Energy Environ. Sci.* **2015**, 8, 2250.
- [20] S. M. Niu, Y. Liu, S. H. Wang, L. Lin, Y. S. Zhou, Y. F. Hu, Z. L. Wang, *Adv. Funct. Mater.* **2014**, 24, 3332.
- [21] Z. L. Wang, *Nano Energy* **2020**, 68, 104272.
- [22] Z. L. Wang, A. C. Wang, *Mater. Today* **2019**, 30, 34.
- [23] a) J. H. Nie, Z. W. Ren, L. Xu, S. Q. Lin, F. Zhan, X. Y. Chen, Z. L. Wang, *Adv. Mater.* **2020**, 32, 1905696; b) J. H. Nie, Z. M. Wang, Z. W. Ren, S. Y. Li, X. Y. Chen, Z. L. Wang, *Nat. Commun.* **2019**, 10, 2264.
- [24] a) F. Zhan, A. C. Wang, L. Xu, S. Lin, J. Shao, X. Chen, Z. L. Wang, *ACS Nano* **2020**, 14, 17565; b) Z. H. Lin, G. Cheng, S. Lee, K. C. Pradel, Z. L. Wang, *Adv. Mater.* **2014**, 26, 4690.
- [25] a) R. H. Wu, L. Y. Ma, C. Hou, Z. H. Meng, W. X. Guo, W. D. Yu, R. Yu, F. Hu, X. Y. Liu, *Small* **2019**, 15, 1901558; b) R. H. Wu, L. Y. Ma, A. Patil, Z. H. Meng, S. Liu, C. Hou, Y. F. Zhang, W. D. Yu, W. X. Guo, X. Y. Liu, *J. Mater. Chem. A* **2020**, 8, 12665.
- [26] a) J. Zhao, W. Zhu, X. Wang, L. Liu, J. Yu, B. Ding, *ACS Nano* **2020**, 14, 1045; b) Z. Li, M. Zhu, J. Shen, Q. Qiu, J. Yu, B. Ding, *Adv. Funct. Mater.* **2019**, 30, 1908411.
- [27] a) R. H. Wu, L. Y. Ma, S. Liu, A. B. Patil, C. Hou, Y. F. Zhang, W. Zhang, R. Yu, W. D. Yu, W. X. Guo, X. Y. Liu, *Mater. Today Phys.* **2020**, 15, 100243; b) L. Ma, R. Wu, H. Miao, X. Fan, L. Kong, A. Patil, X. Y. Liu, J. Wang, *Text. Res. J.* **2020**, 91, 398; c) L. Y. Ma, R. H. Wu, A. Patil, S. H. Zhu, Z. H. Meng, H. Q. Meng, C. Hou, Y. F. Zhang, Q. Liu, R. Yu, J. Wang, N. B. Lin, X. Y. Liu, *Adv. Funct. Mater.* **2019**, 29, 1904549.